Biogeosciences Discuss., 5, 3091–3122, 2008
www.biogeosciences-discuss.net/5/3091/2008/

Biogeosciences Discussions

Biogeosciences Discussions is the access reviewed discussion forum of *Biogeosciences*

Estimating carbon emissions from African wildfires

V. Lehsten[1], K. J. Tansey[2], H. Balzter[2], K. Thonicke[3], A. Spessa[4], U. Weber[5], B. Smith[1], and A. Arneth[1]

[1]Department of Physical Geography and Ecosystems Analysis (INES), Geobiosphere Science Centre, Lund University, Sweden
[2]Centre for Environmental Research, Department of Geography, University of Leicester, UK
[3]Potsdam Institute for Climate Impact Research (PIK) e.V., Potsdam, Germany
[4]Walker Institute for Climate System Research, Department of Meteorology, University of Reading, UK
[5]Max-Planck-Institute for Biogeochemisty, Jena, Germany

Received: 18 June 2008 – Accepted: 9 July 2008 – Published: 8 August 2008

Correspondence to: V. Lehsten (veiko.lehsten@nateko.lu.se)

Published by Copernicus Publications on behalf of the European Geosciences Union.

Abstract

Africa is a continent dominated by fire. Vegetation fires, occurring naturally or human-ignited as a land management practice, have a long history in the continent's savannah ecosystems. These fires contribute substantially to the total carbon emissions (e.g. as CO_2, CO, CH_4, Volatile Organic Compounds, Black Carbon) over large parts of the continent.

Many recent attempts to assess the total area burnt and the amount of carbon emitted have been based on satellite remote sensing of active fires. To calculate emissions, the burned area estimates are typically multiplied with emission factors that are specific for each compound and land cover type, or used to distribute output from a biogeochemical model spatially. We developed a technique for estimating carbon emissions using a modelling approach to scale burned area estimates from L3JRC, a map recently generated from remote sensing of burn scars instead of active fires. Carbon fluxes were calculated by the novel fire model SPITFIRE embedded within the dynamic vegetation model framework LPJ-GUESS, using daily climate input.

For the time period from 2001 to 2005 an average area of $195.5 \pm 24 \times 10^4$ km^2 was burned annually, releasing an average of 723±70 Tg C to the atmosphere; these estimates for the biomass burned are within the range of previously published estimates. Despite the fact that the majority of wildfires are ignited by humans, strong relationships with climatic conditions have been identified in savannas worldwide, driving inter-annual variability. Our investigation of the relationships amongst carbon emissions and its potential drivers, available litter and precipitation showed that burned area as well as carbon emissions show a uni-modal response to precipitation with a maximum at ca. 1000 mm annual precipitation for burned area and emissions and a maximum of ca. 1200 mm annual precipitation for litter availability.

1 Introduction

Africans account for 14% of the global population, but contribute only 3% to the total anthropogenic fossil fuel emissions (Williams et al., 2007). However, the role of African ecosystems for the terrestrial carbon cycle and fire emissions is substantial: 20% of the global net primary production (NPP) and 37% of carbon emissions by biomass burning have been attributed to the African continent (Williams et al., 2007), the latter being mostly released by savannah fires with ignition patterns dominated by human land-management. The vast majority of all savannah fires globally occur on the African continent (Williams et al., 2007).

For a natural system in steady-state, carbon dioxide released by fire will be re-fixed by photosynthesis over the ensuing recovery period and therefore not contribute to a large degree to changes in the global atmospheric CO_2 concentration. A different picture emerges, however, when fire is used in the conversion of forests into agricultural land, as much of the carbon in a forest is fixed in stem biomass and remains airborne when the burnt land is subsequently used for the growing of herbaceous or woody crops on short rotation cycles. Vegetation wildfires generate a considerable amount of climatically active greenhouse gas and particle emissions on the African continent (Scholes et al., 1996b) but the seasonal emission patterns and annual estimates are associated with large uncertainties.

The major determinants of the total carbon release from wildfires at regional-continental scales are the total available plant material for burning (including litter), the burning conditions that determine the combustion completeness, and the annual area burned. Several Africa-wide burned area maps have been produced, e.g. GLOBSCAR (Simon et al., 2004), GBA2000 (Tansey et al., 2004), or the product of Barbosa et al. (1999). However, because of the lack of temporal continuity of these products, active fire detection from thermal channels is often used to account for fire emissions in national greenhouse gas inventories, using the hot spot data as a proxy of burned area (Giglio et al., 2006; Smith et al., 2007). Using active fire detections as a proxy

for area burnt and greenhouse gas emission calculations has several drawbacks. The detection is limited by cloud cover obscuring the view, as well as by temporal gaps between satellite overpasses. Both are more problematic for active than for burn scar detection because the time period for detection is longer for burn scars (Kasischke et al., 2003). Tansey et al. (in preparation) showed that 60% of burn scars in a degraded peat swamp forest, comprising patches of intact forest surrounded by large swatch of secondary vegetation that has been heavily impacted by fire and excessive drainage, went undetected by the MODIS thermal anomaly (hotspot) product. The equivalent burnt area per hotspot detected was between 12 and 15 ha. In a similar study, Smith et al. (2007) calculated a hotspot probability detection rate of only 13% in agricultural fields in southwestern Australia. The successful detection of an active fire depends on reasonably cloud and smoke free conditions, fire intensity, flame front size and algorithm sensitivity, not to mention these conditions prevailing at the exact time that the satellite(s) pass overhead, e.g. four times a day in the case of MODIS AQUA and TERRA.

To estimate fire-induced greenhouse gas emissions from the extent of burned area requires knowledge of the total amount and type of biomass burnt and of trace-gas specific emission factors. In the approach presented here, we simulate fire CO_2 emissions using a modelling system consisting of the dynamic vegetation model LPJ-GUESS (Smith et al., 2001; Sitch et al., 2003) and the fire model SPITFIRE (Thonicke et al., 2008[1]), while prescribing burned area based on the daily global burned area database L3JRC (Tansey et al., 2008). To our knowledge, the only comparable work which also combines satellite derived fire data with a biogeochemical model is the GFED data base by van der Werf et al. (2006) that is based on burned area estimates from active fire data combined with a biogeochemical model (CASA) driven by meteorological data and satellite sensed information on the Normalised Difference Vegetation Index (NDVI)

[1]Thonicke, K., Spessa, A., Prentice, C., Harrison, S. P., and Carmona-Moreno, C.: The influence of vegetation, fire spread and fire behaviour on global biomass burning and trace gas emissions, Glob. Change Biol., submitted, 2008.

as well as vegetation continuous fields (http://glcf.umiacs.umd.edu/data/vcf/). Our approach is unique because we use a recent burned area product for Africa in combination with a detailed vegetation model that accounts for landscape-scale heterogeneity and vertical structure of vegetation, which are important factors determining the burning characteristics as well as fuel loads. The input data to the model are observed, gridded meteorological and soil data.

This study gives us the opportunity to highlight typical areas of uncertainty that recent combined remote sensing/modelling approaches have when calculating pyrogenic emissions. Our goal is to investigate for the period 2001 to 2006 the seasonality and inter-annual variation in fire activity and emissions from vegetation fires over the whole continent. Aiming to identify some of the chief processes that drive this variation we analyse how the hypothesized drivers of wildfires, mean annual precipitation and litter are related to burned area and fire emissions.

2 Materials and methods

2.1 Burned area – L3JRC

The L3JRC burnt area product as described in Tansey et al. (2008) is based on SPOT VEGETATION S1 reflectance data, available nominally on a global, daily, basis and corrected for atmospheric transmissibility using the Simplified Method for Atmospheric Correction (SMAC) code (Rahman and Dedieu, 1994). Observations of the ground were restricted to satellite view zenith angles of less than 50.5 degrees and areas of snow, smoke, cloud, cloud shadow and a sun shadow, the latter produced from the GTOPO 30 global digital elevation model (http://edc.usgs.gov/products/elevation/gtopo30/gtopo30.html), were masked. The burned area algorithm in L3JRC makes use of a temporal index in the 0.83 μm (near infrared, NIR) channel that has the advantage of being highly sensitive to the photosynthetic activity of vegetation (see Tansey et al., 2008 for further information). Post-processing of the data serves to utilize the

latest land cover information to remove some over detections believed mainly to be due to the multi-annual detection of leaf-off conditions in temperate regions and lake melt at high northern latitudes. For the detailed analysis of burnt area, the maps were re-projected into Goodes Interrupted Homolosine equal area projection with a pixel spacing of 1 km. The L3JRC product has been evaluated using 72 Landsat Thematic Mapper (TM) scenes. Fourteen of these images are situated on the African continent. A comparison between the burnt area detected by L3JRC and the burnt area detected by Landsat TM was made between two specific time period (i.e. dates). Landsat TM is considered to give better burnt area estimates because of a superior spatial resolution (30 m), however its temporal resolution and spatial coverage is poor compared to L3JRC. The correlation between burned areas over a standardized equal area grid was computed to derive correlation gradient, intercept values and standard deviations around a best fit line.

The burnt area estimates were corrected for the bias introduced by low-resolution observations and also the standard deviation observed around the best-fit line when compared to a number of Landsat TM images. This correction is necessary because of the calculated underestimation of burnt area due to low spatial resolution of the L3JRC product. The following assumptions were made: In both hemispheres, approximately 60% of the burning activity occurs in vegetation that is described in the Global Land Cover (GLC) 2000 product as being broadleaved or deciduous tree or shrub cover of various degrees of openness in reasonably equal portions. The remainder of the burnt area is spread across five other land cover types. From an earlier validation exercise (Tansey et al., 2008), we know that for tree and shrub cover classes the underestimation of burnt area is approximately 48% and 35% respectively. Hence, assuming that 60% of the total area burnt is on average underestimated by 42% we can derive a more accurate estimate of the true scale of burning. Furthermore, we corrected for the standard deviation (2 s.d.) that we observe in these two land cover types which are both close to 8%. No correction was applied to other land cover types, which make up 40% of the remaining vegetation cover that is burnt. The observed underestimation of

over 40% (Tansey et al., 2008) informs us that the true scale of burning across Africa is greater than we can easily measure using 1 km resolution satellite sensors.

2.2 LPJ-SPITFIRE-DGVM

To simulate potential vegetation we use the dynamic vegetation model LPJ-GUESS (Smith et al., 2001; Sitch et al., 2003) including the fire model SPITFIRE (Thonicke et al., 2008[1]). LPJ-GUESS simulates potential vegetation as a mixture of plant functional types (PFTs) defined by growth form, phenology, life-history characteristics and bioclimatic limits for establishment and survival. Photosynthesis, respiration, tissue turnover and carbon allocation to leaves, fine roots and stems are modeled on an individual basis. The photosynthesis scheme is a modified Farquhar scheme that accounts for adjustment of leaf nitrogen and carboxylation capacity seasonally and within the canopy profile (Haxeltine and Prentice, 1996). Stomatal conductance is related to photosynthesis and soil water availability via an empirical parameterization of boundary layer conductivity (Huntingford and Monteith, 1998). Height and diameter growth are regulated by carbon allocation, conversion of sapwood to heartwood, and a set of prescribed allometric relationships for each PFT. Soil organic matter dynamics (four pools) follows first-order kinetics with a decay rate that is sensitive to temperature (modified Arrhenius) and soil water content (Sitch et al., 2003). The version used in this study includes improved representations of ecosystem hydrological cycling as documented by Gerten et al. (2004). The model framework can be applied in global "population" mode that is based on a computationally efficient, comparatively simple interaction between the model's plant functional types (Sitch et al., 2003) or – as applied here – in "cohort"-mode that represents the vegetation of a given modeled area or gridcell by a number of patches in different stages of recovery or succession following disturbance, and within each patch by cohorts that differ in age and related growth characteristics (Smith et al., 2001). Establishment, mortality and competition among neighboring individuals for light and soil resources are taken into account explicitly. To account for the heterogeneity resulting from population processes, which are modeled stochastically,

the vegetation coverage of a grid-cell is taken as the average among the replicated patches (Smith et al., 2001). The model is driven by atmospheric CO_2 concentration, temperature, precipitation, radiation, and soil physical properties. For this study, burned area as detected by L3JRC was also read in. The burned area map of L3JRC has an original grid spacing of 1 km and was converted to daily burned fractions per 1 degree grid cell, the spatial resolution of the climate input (see Model experimental setup below). The model runs at daily time step.

Fuel combustion in SPITFIRE depends on the amount of fuel, the relative proportions of fuels in different size classes (leaves and twigs, small branches, large branches and trunks), and the moisture content of fuels and follows Peterson and Ryan (1986). The calculation of the latter is based the Nesterov index (Nesterov, 1949) which accumulates on each subsequent day with precipitation below 3 mm and is reset to zero after a 3 mm precipitation event. We followed previously used approximations (Venevsky et al., 2002; Thonicke et al., 2008[1]) of the dew point temperature which is required to calculate the Nesterov Index being the daily minimum temperature minus 4 K (Running et al., 1987). Since the burned area was prescribed from a burned area product rather than fire hot spots, the exact timing of the fire event was unknown; it could have happened any time between last non-detection and first detection of the burn scar which may be separated by a several days lag. This opens the possibility for burn scars being detected for the first time on rainy days, which would reset the Nestorov Index in the SPITFIRE calculations which, in turn, would lead to an underestimation in of the Nesterov Index required for further calculations. In these cases, scorch height and fuel combustion were calculated taking the maximum Nesterov Index of the week preceding the detection of the burn scar.

Fire intensity in SPITFIRE is explicitly simulated as the product of the calorific content of the fuel, the amount of fuel consumed and the rate of spread of the fire front (based on Byram, 1959; Rothermel, 1972; Wilson, 1982; Pyne et al., 1996). It depends on climatic conditions as well as on the type and amount of available fuel produced by the vegetation (Thonicke et al., 2008[1]). Above-ground litter simulated in LPJ-GUESS-

SPITFIRE is separated into different size classes (leaves and twigs, small branches, large branches and trunks) as constant ratios from the total wood amount of (0.045, 0.075, 0.21 and 0.67 respectively; Thonicke et al., 2008[1]). These classes capture the way the moisture content of different sized fuels respond with ambient conditions based on the surface-area-to-volume ratio (Pyne et al., 1996). For instance, tree and grass leaf litter has a large surface-area-to-volume ratio, thus equilibrating relatively quickly to changing prevailing atmospheric moisture conditions and supporting intense fires of short duration. Due to their rapid drying response to higher temperatures and/or lower relative humidity, fine fuels are generally totally consumed by most fires and as a result, fine fuel fires spread very quickly. By contrast, the fuel classes representing dead stem wood respond less rapidly to changes in ambient moisture conditions because they have a smaller surface-area-to-volume ratio. While coarse litter does not normally affect rate of spread of fires, when conditions are sufficiently dry e.g. during the late dry season or droughts, they become increasingly available for combustion, and as a result, they play an increasing role in determining the rate of spread and fire intensity.

Instead of updating carbon pools annually, which is the standard procedure within the LPJ-GUESS framework (Smith et al., 2001), here we chose a daily update of litter carbon pools. If the ratio between water supply and water demand by raingreen trees is below 0.35 for more than 30 days (grasses 7 days respective) leaves are shed and added to the litter pool. The litter decomposition was separated between wood and leaf litter with turnover times at 10°C of 2.85 years for leaf litter and 20 years for wood litter (turnover times decline with temperature following a modified Arrhenius relationship; Sitch et al., 2003).

All calculations in the module SPITFIRE are based on these daily values of litter availability. The emissions of carbon by wildfires are subsequently calculated by multiplying the burned area with the amount of available litter in the burnt area, with the overall combustion depending on the litter type and burn conditions as described above.

Imposing a size dependent mortality has been identified as one of the key factors for correctly modelling the effects of wildfires on savannah vegetation by Hanan et

al. (2008). In SPITFIRE the effect of fires on tree survival depends on the degree of crown and cambial damage (Thonicke et al., 2008[1]). The proportion of the crown affected by fire depends on crown architecture, the scorch height of the fire, and the resistance of different PFTs to crown scorching. Scorch height is a non-linear function of fire intensity and is PFT-specific. Cambial damage depends on the residence time of the fire and bark thickness, which is a function of tree diameter and is also PFT-specific (Thonicke et al., 2008[1]). This captures the generally observed fire-induced mortality dynamics whereby small trees (i.e. young age cohorts) are more likely to be affected by crown scorching and cambial damage than older and taller trees. In this way, the fire simulation imposes a size dependent mortality on vegetation which, in turn, changes the ratio of tree to grass, the age distribution of trees and thus, fuel production and the propensity for fire in the following year.

In order to improve the representation of savannah vegetation dynamics in LPJ-GUESS, a minimum available soil moisture level for tree establishment was introduced, following Miller et al. (2008). By increasing the ratio between stem diameter and tree height for tropical broad-leafed rain-green trees (values based on measurements of *Acacia senegal* in Demokeya, Sudan, Bashir Awad El Tahir, unpublished) a more realistic tree density was achieved. Fire-related PFT parameters, like susceptibility to crown scorching or cambial damage and fuel bulk density were set as in Thonicke et al. (2008[1]), except for tropical broadleaf rain-green trees. Here the mortality experienced after complete crown scorching was increased from 5% to 87% corresponding to the average stem mortality found for deciduous trees after an intense fire by Williams et al. (1998). The mortality caused by cambial damage was reduced to zero since it is known that these trees suffer very low fire related mortality as long as their crown is not scorched (Hanan et al., 2008). We are not aware of measurements of fuel bulk densities of litter generated by tropical raingreen trees and applied the value for the tropical broad leafed evergreen tree as used in (Thonicke et al., 2008[1]) which is based on Williams et al. (1998).

2.3 Model experiment setup

LPJ-GUESS-SPITFIRE was here applied on a 1×1 degree grid across Africa. 100 patches of 1000 m^2 were simulated for each gridcell, to account for stochastic processes (see model description above). The scale at which fires normally occur is larger than the scale of a single simulated patch, and the fractional area burned each year, as detected by L3JRC, can be assumed to be equal to the probability with which any particular point burns entirely. By simulating multiple patches at each grid cell and subsequently averaging, we ensure not only that the area burned within SPITFIRE closely matches the burned area detected by L3JRC but also that effects on vegetation structure, like tree age and spacing are represented realistically (see Fig. 1).

The climate data set covered the period from 1979 to 2006, hereinafter referred to as the "target period". Temperature and global radiation were obtained from NCEP re-analysis II data (Kalnay, 1996) and averaged to daily values. Precipitation was derived by adjusting NCEP re-analysis II data with CRU data (CRUTS2.1, Mitchell and Jones 2005 plus a complimentary data set the year 2003 based on the same techniques as Mitchell and Jones, 2005) and TRMM data (Kummerow et al., 1998) according to their overlap period. For the TRMM period (1998–2006), a monthly correction factor between NCEP re-analysis II data and TRMM data was applied. For the period prior to TRMM (1979–1997) precipitation was corrected based on a monthly correction factor between CRU data with NCEP re-analysis II data, and an additional monthly mean correction factor between TRMM data and CRU data (1998–2003). This decreased overall precipitation by 15.2%. The simulations started with a spin up of 1000 years to achieve vegetation structure and soil carbon pools in approximate steady state with climate at the beginning of the target period. To account for the effects of inter-annual variability in climate on vegetation and soils, the spin up phase of the simulations was driven by continuous cycling of the climate time series for the target period. The CO_2 level was kept constant throughout the spin up at the 1982 level of 341.13 ppm, which is the level stipulated in the CarboAfrica Model Intercomparison protocol (Weber et al.

2008[2]) and increased during the target period according to measurements at Mauna Loa (www.esrl.noaa.gov/gmd/ccgg/trends/).

2.4 Analysis of the relationships between precipitation, burned area, litter and emissions

Since the fire season is shifted by six months between northern (NHA) and Southern Hemisphere Africa (SHA), we related burned area, emissions and litter to the precipitation which occurred in the 365 days before the peak of the fire season for each year (NHA: 15 March Mar; SHA: 15 September).

For each grid cell, the arithmetic mean of the precipitation, leaf litter, emissions and burned area were calculated over the 6 years considered in this study. A scatter plot was generated and a generalized linear model (GLM) was fitted between the independent and the response variable applying a logit transformation to the response data, and assuming binomial error structures. The logit transformation requires the dependent variable to be bounded between zero and one (Dobson, 2002), which is the case for ratios like the burned area. In cases where the response variable was not a ratio (leaf litter, emissions) the values were transformed to proportions of an arbitrary maximum value by dividing by 10 kg for leaf litter and 1kg for emissions (see Fig. 6). The (logit) transformations of the response variable V is:

$$\text{logit}(V) = \log_e(V/(1 - V)) \quad (1)$$

Values of V which were equal to 0 were set to 0.00001. The GLMs contained a linear and a quadratic term of the predictor variable. The coefficient of determination (r^2) was calculated by back-transforming the modelled values

$$V = 1/(1 + e^{\text{logit}(V)}) \quad (2)$$

[2]Weber, U., Jung, M., Reichstein, M., Beer, C., Braakhekke, M., Lehsten, V., Ghent, D., Kaduk, J., Viovy, N., and Ciais, P.: Interannual variability of the terrestrial African carbon balance – a model-intercomparison study, Biogeosciences Discuss., submitted, 2008.

for the data which was used to estimate the GLM and regressing them on the observed values. The derivation of the parameters for the GLMs was performed according to Dobson (2002). Fitting GLMs to the data (i) allows the general trend as well as the shape of the relationship to be examined, which would otherwise be difficult given the amount of data points in the scatter plot, and (ii) shows the strength of the relationship, since it enables us to calculate a coefficient of determination (r^2-value).

3 Results

3.1 Burned Area – L3JRC

The frequency and spatial extent of L3JRC burnt area within the sub-Sahara region of Africa is shown in Fig. 2, covering seven fire years between 1 April 2000 and 31 March 2007. Two main regions of burning activity can be identified where fires occur on an almost annual basis. The first is a region in Sudan, Chad and Ethiopia, the second covers parts of D.R. Congo, Angola, Tanzania and Mozambique. The potential vegetation simulated by LPJ-GUESS-SPITFIRE for these areas mainly consists of drought-deciduous forests and woodlands (not shown, Lehsten et al., in preparation). The productivity in these areas is strongly related to precipitation: an increase in precipitation results in a replacement of the deciduous vegetation by evergreen forest according to the model (not shown., Lehsten et al., in preparation). However, large parts of these areas are used for agriculture and grazing resulting in a high potential for human ignition.

Estimates of burnt area, productivity and pyrogenic carbon release are given for the area north and south of the equator in Table 1, separated into the six years covered by L3JRC.

3.2 Fire seasonality and total carbon emissions

The fire season of the Northern Hemisphere peaks in March, with very low fire activities from June to January, while in the southern part of the continent the peak lies in October

with the main activity from August to January (see Fig. 3).

The calculated total amount of biomass burned for the entire continent was 723±70 Tg C a^{-1} over the period 2001–2006 (612±40 Tg C a^{-1} prior to the correction of burned area by vegetation class from the GLC2000 product) (Table 1). Given the ecosystem model estimate of continental net primary production of 9.0±0.7 Pg C a^{-1}, more than 8% of biomass produced annually is consumed by wildfires. Areas with the highest NPP, up to and above 1 kg C m^{-2} a^{-1} (Fig. 4), were located in the rain forest region around the equator that contributes only a very small proportion to the fire emissions (Fig. 5). When restricting the analysis to savannah, deciduous and xeric forest ecosystems, defined as areas with a leaf area index (LAI) of tropical rain-green trees above 0.5 according to Hickler et al. (2006), a total of 10% of NPP would be consumed by wildfires annually (savannah NPP=7.2±0.62 Pg C a^{-1}; emitted carbon=719±70 Tg C a^{-1}).

While the total burned area differed by approximately 20% between the southern and Northern Hemisphere of the continent, the calculated carbon emissions in SHA exceeded emissions in NHA by up to 40% (Table 1, Fig. 5). Naturally, hemispherical fire emissions in northern Africa are constrained by the extension of the Sahara desert but Fig. 5 also shows areas with a larger concentration of grid cells with high emissions on a per area basis in the SHA.

3.3 Inter-annual variation

Total burned area over the simulation period varied inter-annually by ca. 33% whereas the total vegetation emissions differed by 24%, or 32% (not shown) in the case of savannahs, deciduous and xeric forests only (Table 1). These values were higher than the inter-annual range for precipitation (20%), and also for total (21%) and savannah, deciduous and xeric forest (17%) NPP. As expected, annual precipitation was well correlated with NPP (r^2=0.91; n=6, Table 1) with highest NPP in the wettest (2006) and lowest NPP in the driest year (2005). Although the magnitude of the inter-annual variation was different for area burnt vs. precipitation and NPP, the pattern of year to

year variation in simulated total carbon emissions follow approximately the variation in burned area in both hemispheres (r^2 values: SHA 0.81; NHA 0.75; total 0.79; n=6; Table 1).

3.4 Relationships between precipitation, litter, burned area and emissions

Precipitation and burned area showed a non-linear relationship, with highest values of burned area located in regions with approximately 1000 mm annual precipitation (Fig. 6a). A similar pattern was detected in the relationship between precipitation and annual fire emissions (Fig. 6b), and between precipitation and available litter, although for the latter the highest litter production was slightly shifted to higher precipitation (Fig. 6c).

By contrast to relationships with annual precipitation, the highest annual emissions tended to be associated with gridcells which burn each year by with a spatial coverage of approximately 40% (Fig. 6d). Areas with lower, but also with higher burning frequency result in lower annual emissions. At the same time, areas with high burned area tend to have only low litter accumulation compared to grid cells with a lower amount of burning (Fig. 6f).

It is apparent in Fig. 6e that some areas may have a lower amount of leaf litter produced over a year than is emitted in fires, although on an average (the red line of the modelled response) the emission is lower than the leaf litter. Although green biomass and standing dead wood also contribute to emissions, this apparent discrepancy mainly reflects the influence of litter decomposition, which reduces the reported litter pool in the output of the model.

The fitted GLM parameter values as well as the coefficients of determination (r^2 values) for each relationship are given in the figure caption (Fig. 6). The strongest coefficient of determination was found between burned area and emissions (r^2=0.66) followed by the relationship between precipitation and litter (r^2=0.63). A combined GLM in which burned area and litter are used as predictors for annual emissions results in a coefficient of determination (r^2-value) of 0.75 (logit (E)=–6.5+14.7×BA–

$15.7 \times BA^2 + 156 \times Lit/10 - 2314 \times (Lit/10)^2$) (not shown).

Generating these GLMs with other litter classes than leaf litter or with total litter, resulted in lower r^2 values (data not shown), indicating that leaf litter had the highest influence on emissions in the simulations.

4 Discussion

We use a remote sensing product to prescribe burnt area and to investigate climate-vegetation interactions, particularly in terms of NPP and litter production on fire carbon emissions in Africa. Published estimates of burned biomass at the African continent are available for the entire continent, or Southern Hemisphere Africa, and vary considerably among studies (Williams et al., 2007; Korintzi, 2005). The L3JRC plus LPJ-GUESS-SPITFIRE estimates are well within the continental range of 300 to 1800 Tg C a^{-1} (Williams et al., 2007), and the SHA range of 174 to 1200 Tg C a^{-1} (Korontzi, 2005). An inter-annual variability of fire-related carbon emissions (1985–1991) was reported in Barbosa et al. (1999) for Southern Hemisphere Africa, using images of the advanced very high resolution radiometer with a 5 km resolution. A map of the main vegetation classes was further used to assign biomass density, combustion efficiency and emission factors to each biome which were modified by weekly values of NDVI, which were derived from the same remote sensing product. Their value of 50% was larger than the 34% calculated in our study although the differences in methodology as well as in the in time periods makes a direct comparison difficult. Overall, we consider our estimates of burned biomass as rather conservative owing to the use of precipitation at relatively coarse resolution (2.5 degree grid from NCEP, Kalaney 1996), the assumption of homogenous precipitation within a grid cell may lead to an underestimation of fuel dryness.

In the comprehensive study of global biomass burning by van der Werf et al. (2006), an estimated total fire emissions from SHA of 576±72 Tg C a^{-1} were associated with a burned area of $79.3 \pm 9.6 \times 10^4$ km^2. These values are in the same range as an earlier

calculation by van der Werf et al. (2003) based on the same biogeochemical model, but for a single year only and with different driving data. For NHA, $627 \pm 75\,\mathrm{Tg\,C\,a^{-1}}$ were emitted from a burned area of $142.5 \pm 12.3 \times 10^4\,\mathrm{km^2}$; excluding the Mediterranean regions. While our estimates of the emissions and burnt area are relatively comparable with the results from van der Werf et al. (2003, 2006) for SHA, they differ substantially for the northern part of the continent. Aside from differences in the calculated productivity (see below) this discrepancy might be explained by the proportionally larger burned area in NHA compared to SHA inferred by van der Werf (2006). The L3JRC detections assign a significantly lower burnt area in NHA than SHA even though the Mediterranean areas are included.

The analysis of van der Werf et al. (2006) uses burned area estimates of Giglio et al. (2006) based on active fire data (hotspots). A regression tree described the relationship between active fire counts and burned area, relating burned area per active fire count and vegetation continuous fields as well as cluster size for a number of example areas. The amount of burned area assigned to each detected active fire ranges from areas below the size of the fire active fire pixel (0.1–$0.2\,\mathrm{km^2}$) up to $5.5\,\mathrm{km^2}$ (SHA) or $6\,\mathrm{km^2}$ (NHA) and is indicative for the uncertainty connected with estimating burned areas from active fire data.

The L3JRC burnt area is based on the detection of burn scars which should provide more accurate information than hot spots since the potential overpasses of the satellite that lead to a successful detection are more frequent for a burn scar than for an active fire. Still, in some regions the detected burn scars are likely to be underestimated which was accounted for in the overall calculations by applying the required corrections.

The vast majority of fires in Africa are ignited by humans (Saarnak, 2001) as part of grazing management and agricultural activities, who may choose dry periods for ignition. SPITFIRE distinguishes anthropogenic and lightning ignition sources to calculate burnt area but these are complex to parameterise and are being investigated in a separate study (Lehsten et al., in preparation). Using a global parameterisation of human ignition, Thonicke et al. (2008[1]) calculate a burnt area of $117 \pm 14 \times 10^4\,\mathrm{km^{-2}}$ in NHA

and $198 \pm 18 \times 10^4$ km^{-2} in SHA (mean value for 1997–2002±standard deviation). The calculated area burnt is larger compared to the L3JRC product, but lies in the range of the estimates of our study. Their study also assigns more burned area to the southern than to the Northern Hemisphere of the African continent as estimated in the L3JRC product. While this is not part of the analysis here, adopting a suitable parameterisation for human ignition patterns based on population distribution and life-style is an important task which will be the focus of future analysis.

Variation in NPP affects fuel load and thus the amount of biomass that can be combusted and sustain fire spread. The total amount, distribution and processes driving year-to-year variability in NPP therefore constitute a further major uncertainty in the estimation of African fire emissions. In a study by Scholes et al. (1996a), burned area and biomass estimates from remotely sensed NDVI and hot spot data were combined with a functional vegetation type classification with respect to the fire regime. Fuel load in this approach was estimated from mean annual precipitation and vegetation. Their estimate of biomass burned for SHA, 45–132 C a^{-1} (90–264 Tg DM a^{-1}) in the year 1989, is much lower than our estimate of between 379 and 580 Tg C a^{-1} for the six-year period 2001–2006.

Another approach to quantify African wildfire emissions area is to use remotely sensed fire radiative energy as a proxy for combustion completeness instead of an estimate based on climatic conditions and fuel composition as applied in this study. In a recent quantification of carbon emissions over the African continent for the time between February 2004 and January 2005 Roberts et al. (2008[3]) estimated the total carbon emission for one year to be above 402 Tg C (855 Tg dry mass). The authors consider their estimate to be a too low estimation of the carbon emission. Though considerably lower than our estimate of 718 Tg C for 2004 it indicates that the correct value should be in the same order of magnitude since both methods use different remote sensing data and rely on different models to estimate carbon emissions.

[3]Roberts, G., Wooster, M. J., and Lagoudakis, E.: Annual African Biomass Burning Temporal Dynamics, Biogeosciences Disucss., in review, 2008.

Van der Werf et al. (2006) used a biogeochemical model (CASA) to calculate NPP and fuel loads available for burning, driven by remotely sensed NDVI, and climate data. Their mean NPP of 13 Pg C a^{-1} is at the upper end of published estimates, 7 to 13 Pg C a^{-1} (Williams et al., 2007). The lower NPP calculated with LPJ-GUESS, 9.0 Pg C a^{-1} over the simulation period, is one of the reasons for the lower estimated continental emission of carbon in this study compared to van der Werf et al. (2006), even though the L3JRC burned area is larger.

Differences in NPP calculation between the two models are likely also the main reason for different estimates of the average emissions when expressed on a per burned area basis. Whereas van der Werf (2006) estimated emissions of 441 g C m^{-2} a^{-1} for NHA and 734 g C m^{-2} a^{-1} for SHA, our estimates were 318 g C m^{-2} a^{-1} and 414 g C m^{-2} a^{-1} respectively. Therefore, while both studies arrived at higher average emissions for SHA, their regional totals differ by up to 70%.

The seasonal pattern of wildfire emission may be evaluated using estimates of CO emissions derived from satellite remote sensing (Andreae and Merlet, 2001). Besides annual totals, the correct seasonality of burning is crucial to eventually link gross fire emissions to production of atmospheric agents like O_3 and aerosols. Fire combustion completeness plays a major role since it varies with fuel type, and fuel moisture content. The calculated wildfire emissions will therefore depend strongly on the timing of ignition, since the fuel availability as well as the moisture content changes with time of the year. For SHA, CO fluxes derived from the Measurements Of Pollution In The Troposphere (MOPITT) sensor peak in September (Andreae and Merlet, 2001; van der Werf et al., 2006). The sensor signal peak precedes L3JRC burnt-area peak as well as peak in fire emissions simulated by LPJ-GUESS-SPITFIRE by about one month. An explanation for this could be that areas with maximal litter combustion burn early in the fire season. L3JRC records burned areas which are not detected at the time of burning but at the next satellite overpass with suitable viewing conditions, which may also add to the delay. Previous calculations of the seasonality have, by contrast to the present study, preceded the satellite signal notably (van der Werf et al., 2006). The reasons for

the remaining one-month discrepancy await further exploration.

The relationship between burned area and precipitation for African savannahs is similar to a uni-modal relationship between mean annual precipitation and the proportion of area burned for the wet-dry tropics of northern Australia (Spessa et al., 2005). There, the maximum of burned area was around 1200 mm annual precipitation, and mean proportion of burned area at this maximum was somewhat higher (0.28 vs. 0.2 in our study). These observations indicate a strong similarity in the functional properties of savannahs in different parts of the world that emerge in converging cross-continental patterns. One important process in this context is precipitation being an important driver not only for NPP but also for litter (2007) production and thereby fuel load (Fig. 6c, r^2=0.63), as demonstrated also at the site level by Hely et al. (2007). In our simulations, the relationship between leaf litter and the calculated emissions was relatively weak (Fig. 6e, r^2=0.37). Two reasons for this are likely: (i) wet regions also accumulate litter, but either do not burn as frequently as expected from their fuel load alone, or if they burn, their lower combustion efficiency results in low emission rates per amount of litter combusted; (ii) areas with high proportion of burned area per year (Fig. 6f) tend to have low fuel loads. Here fuel can not accumulate over longer periods due to the frequent burning: in the model results, emissions decline for burned areas that are proportionally larger than 0.4 (Fig. 6b). However, burned area and available litter taken together resulted in a higher coefficient of determination than using burned area as the sole predictor of carbon emissions, indicating the importance of both factors for emissions.

Sankaran (2004) classifies savannah vegetation models according to the key process which enables the co-existence of grasses and trees. Although LPJ-GUESS-SPITFIRE contains several features which have been shown (in other studies) to facilitate such a co-existence, such as differences in the rooting niche as well as in phenology, the most important process for maintaining savannah vegetation is the demographic bottleneck caused by wildfires. Switching off fires in the simulations results in a very narrow transition zone between pure forest and pure grasslands (Lehsten et al.,

in preparation), which is in accordance with Sankaran et al. (2004).

5 Conclusions

Our estimates of burnt area and biomass for sub-Saharan Africa are within the range of previous estimates and the simulated seasonal burn peak (October) is close to the satellite derived CO maximum (September) for Southern Hemisphere Africa. Using a dynamic vegetation model allowed us to characterise the strongly non-linear relationships among precipitation, NPP and litter production as the main drivers of fire emissions, yielding some general patterns that might be representative for savannah ecosystems globally.

Burned biomass is a parameter which can feed into carbon emission inventories as required under the Kyoto Protocol and is also required to simulate the non-carbon emissions from wild fires that are important for our understanding of tropospheric chemistry. Combining satellite-generated burned area maps with vegetation modelling provides the opportunity to evaluate processes underlying inter-annual variation in fire that are largely driven by climate-productivity interactions. A next step will be to investigate effects of human vs. natural (lightning) ignition patterns and to develop projections and hindcasts of future and past fire patterns that are based on climate and socio-economic drivers.

Acknowledgements. The work was supported by the European Commission via the FP6 project CarboAfrica. We thank Bashir Awad El Tahir for providing the vegetation parameters for savannah trees. The L3JRC production team, Jean-Marie Grégoire, Pierre Defourny, Roland Leigh, Jean-François Pekel, Eric van Bogaert, Etienne Bartholomé, José M. C. Pereira, Ana Barros and João Silva are acknowledged. Colin Prentice contributed to the development of the SPITFIRE model.

References

Andreae, M. O. and Merlet, P.: Emission of trace gases and aerosols from biomass burning, Glob. Biogeochem. Cycle, 15, 955–966, 2001.

Barbosa, P. M., Stroppiana, D., Gregoire, J. M., and Pereira, J. M. C.: An assessment of vegetation fire in Africa (1981–1991): Burned areas, burned biomass, and atmospheric emissions, Glob. Biogeochem. Cycle, 13, 933–950, 1999.

Byram, G. M.: Combustion of forest fuels, in: Forest Fire: Control and Use, edited by: Davis, K., McGraw-Hill Book Company, New York, 61–89, 1959.

Dobson, A. J.: An introduction to generalized linear models, Chapman & Hall/CRC texts in statistical science series, Chapman & Hall/CRC, Boca Raton, 2002.

Gerten, D., Schaphoff, S., Haberlandt, W., Lucht, W., and Sitch, S.: Terrestrial vegetation and water balance – hydrological evaluation of a dynamic global vegetation model, J. Hydrol., 286, 249–270, 2004.

Giglio, L., van der Werf, G. R., Randerson, J. T., Collatz, G. J., and Kasibhatla, P.: Global estimation of burned area using MODIS active fire observations, Atmo. Chem. Phy., 6, 957–974, 2006.

Hanan, N. P., Sea, W. B., Dangelmayr, G., and Govender, N.: Do fires in savannas consume woody biomass? A comment on approaches to modeling savanna dynamics, American Naturalist, 171, 851–856, 2008.

Haxeltine, A. and Prentice, I. C.: A general model for the light-use efficiency of primary production, Funct. Ecol., 551–561, 1996.

Hely, C., Caylor, K. K., Dowty, P., Alleaume, S., Swap, R. J., Shugart, H. H., and Justice, C. O.: A temporally explicit production efficiency model for fuel load allocation in southern Africa, Ecosystems, 10, 1116–1132, 2007.

Hickler, T., Prentice, I. C., Smith, B., Sykes, M. T., and Zaehle, S.: Implementing plant hydraulic architecture within the LPJ Dynamic Global Vegetation Model, Global Ecol Biogeogr, 15, 567–577, 2006.

Huntingford, C. and Monteith, J. L.: The behaviour of a mixed-layer model of the convective boundary layer coupled to a big leaf model of surface energy partitioning, Bound.-Lay. Meteorol., 88, 87–101, 1998.

Kasischke, E. S., Hewson, J. H., Stocks, B., van der Werf, G., and Randerson, J.: The use of ATSR active fire counts for estimating relative patterns of biomass burning - a study from the

boreal forest region, Geophys. Res. Lett, 30(4), 1969, doi:10.1029/2003GL017859, 1969 Artn 1969, 2003.
Kummerow, C., Barnes, W., Kozu, T., Shiue, J., and Simpson, J.: The Tropical Rainfall Measuring Mission (TRMM) sensor package, J. Atmos. Ocean. Tech., 15, 809–817, 1998.
Mitchell, T. D. and Jones, P. D.: An improved method of constructing a database of monthly climate observations and associated high-resolution grids, Int. J. Climatol., 25, 693–712, doi:10.1002/joc.1181, 2005.
Nesterov, V. G.: Gorimost' lesa i metody eio opredelenia., Goslesbumaga, 1949.
Peterson, D. L. and Ryan, K. C.: Modeling Postfire Conifer Mortality for Long-range Planning, Environ Manage, 10, 797–808, 1986.
Pyne, S. J., Andrews, P. L., and Laven, R. D.: Introduction to wildland fire, Wiley, New York, 769 pp., 1996.
Rahman, H. and Dedieu, G.: SMAC: A simplified method for the atmospheric correction of satellite measurements in the solar spectrum, Int J Remote Sens, 15, 123–143, 1994.
Rothermel, R. C.: A Mathematical Model for Predicting Fire Spread in Wildland Fuels, Ogden, Utah, 1972.
Running, S. W., Ramakrishna, R. N., and Hungerford, R. D.: Extrapolation of synoptic meteorological data in mountainous terrain and its use for simulating forest evapotranspiration and photosynthesis, Can. J. Forest Res., 17, 472–483, 1987.
Saarnak, C. F.: A shift from natural to human-driven fire regime: implications for trace-gas emissions, Holocene, 11, 373–375, 2001.
Sankaran, M., Ratnam, J., and Hanan, N. P.: Tree-grass coexistence in savannas revisited - insights from an examination of assumptions and mechanisms invoked in existing models, Ecol. Lett., 7, 480–490, 2004.
Scholes, R. J., Kendall, J., and Justice, C. O.: The quantity of biomass burned in southern Africa, J. Geophys. Res.-Atmos., 101, 23 667–23 676, 1996a.
Scholes, R. J., Ward, D. E., and Justice, C. O.: Emissions of trace gases and aerosol particles due to vegetation burning in Southern Hemisphere Africa, J. Geophys. Res.-Atmos., 101, 23 677–23 682, 1996b.
Simon, M., Plummer, S., Fierens, F., Hoelzemann, J. J., and Arino, O.: Burnt area detection at global scale using ATSR-2: The GLOBSCAR products and their qualification, J. Geophys. Res.-Atmos., 109, D14S02, doi:10.1029/2003JD003622, 2004.
Sitch, S., Smith, B., Prentice, I. C., Arneth, A., Bondeau, A., Cramer, W., Kaplan, J. O., Levis, S.,

Lucht, W., Sykes, M. T., Thonicke, K., and Venevsky, S.: Evaluation of ecosystem dynamics, plant geography and terrestrial carbon cycling in the LPJ dynamic global vegetation model, Glob. Change Biol., 9, 161–185, 2003.

Smith, B., Prentice, I. C., and Sykes, M. T.: Representation of vegetation dynamics in the modelling of terrestrial ecosystems: comparing two contrasting approaches within European climate space, Global Ecol Biogeogr, 10, 621–637, 2001.

Smith, R., Adams, M., Maier, S., Craig, R., Kristina, A., and Maling, I.: Estimating the area of stubble burning from the number of active fires detected by satellite, Remote Sens. Environ., 109, 95–106, 2007.

Spessa, A., McBeth, B., and Prentice, C.: Relationships among fire frequency, rainfall and vegetation patterns in the wet-dry tropics of northern Australia: an analysis based on NOAA-AVHRR data, Global Ecol Biogeogr, 14, 439–454, 2005.

Tansey, K., Gregoire, J. M., Binaghi, E., Boschetti, L., Brivio, P. A., Ershov, D., Flasse, S., Fraser, R., Graetz, D., Maggi, M., Peduzzi, P., Pereira, J., Silva, J., Sousa, A., and Stroppiana, D.: A global inventory of burned areas at 1 km resolution for the year 2000 derived from SPOT VEGETATION data, Clim. Change, 67, 345–377, 2004.

Tansey, K., Gregoire, J. M., Defourny, P., Leigh, R., Pekel, J. F. O., van Bogaert, E., and Bartholome, E.: A new, global, multi-annual (2000–2007) burnt area product at 1 km resolution, Geophys. Res. Lett, 35, 2008.

van der Werf, G. R., Randerson, J. T., Collatz, G. J., and Giglio, L.: Carbon emissions from fires in tropical and subtropical ecosystems, Glob. Change Biol., 9, 547–562, 2003.

van der Werf, G. R., Randerson, J. T., Giglio, L., Collatz, G. J., Kasibhatla, P. S., and Arellano, A. F.: Interannual variability in global biomass burning emissions from 1997 to 2004, Atmo. Chem. Phy., 6, 3423–3441, 2006.

Venevsky, S., Thonicke, K., Sitch, S., and Cramer, W.: Simulating fire regimes in human-dominated ecosystems: Iberian Peninsula case study, Glob. Change Biol., 8, 984–998, 2002.

Williams, C. A., Hanan, N. P., Neff, J. C., Scholes, R. J., Berry, J. A., Denning, A. S., and Baker, D. F.: Africa and the global carbon cycle, Carb. Bal. Manag., 2(3), doi:10.1186/1750-0680-2-3, 2007.

Williams, R. J., Gill, A. M., and Moore, P. H. R.: Seasonal Changes in Fire Behaviour in a Tropical Savanna in Northern Australia, Int. J. Wildland Fire, 8, 227–239, 1998.

Wilson, R. A. J.: A re-examination of fire spread in free burning porous fuel beds, Intermountain Forest and Range Experiment Station, Forest Service, US Dept. of Agriculture, Ogden, Utah, 1982.

Table 1. Burned area, pyrogenic carbon release, net primary productivity (NPP) and precipitation between 2001 and 2006 given as annual totals and mean±standard deviation. SHA=Southern Hemisphere Africa, NHA=Northern Hemisphere Africa.

Year	Area	2001	2002	2003	2004	2005	2006	2001–2006
Burned area [10^4km^2]	SHA	136.1	98.6	113.9	98.7	91.4	112.5	108.5±16.0
	NHA	97.0	81.8	73.5	94.6	73.7	100.6	86.9±12.0
	Total	233.2	180.4	187.5	193.3	165.2	213.2	195.5±24.3
Carbon Release [Tg a^{-1}]	SHA	580	387	482	379	453	413	448± 75
	NHA	277	263	240	339	239	288	274±37
	Total	857	650	722	718	691	701	723±70
NPP savannah, deciduous	SHA	4.1	4.0	3.7	4.0	3.4	4.3	3.9±0.32
and xeric forest [Pg C a^{-1}]	NHA	2.3	2.3	2.4	2.6	2.2	2.5	2.4±0.15
NPP total [Pg C a^{-1}]	Total	9.1	8.9	8.7	9.4	7.9	10.0	9.0±0.7
Total Precipitation [10^4km^3]	Total	1.80	1.83	1.81	1.81	1.55	1.94	1.79±0.13

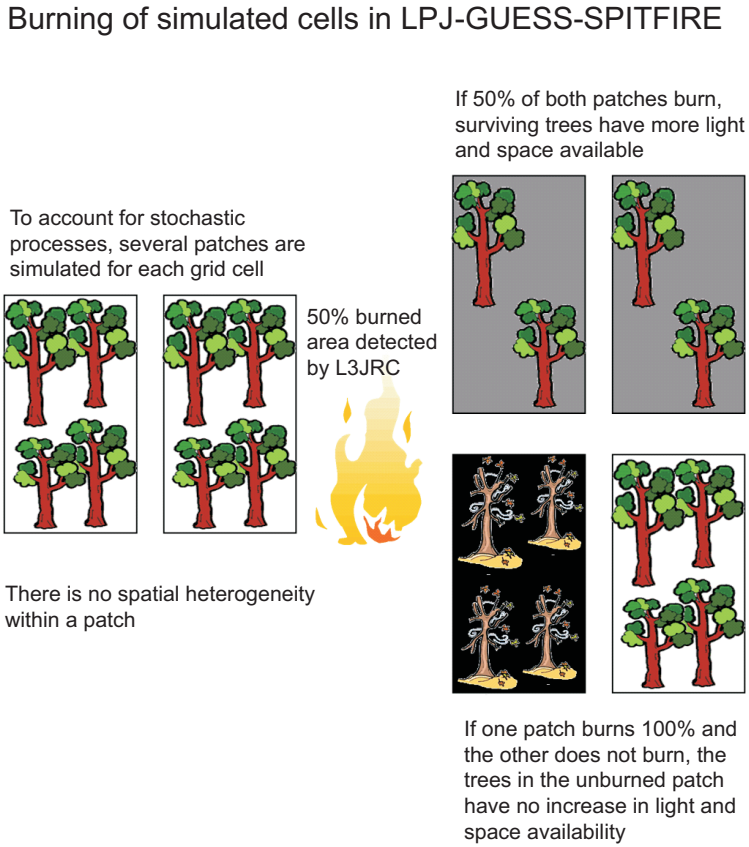

Fig. 1. The representation of burning a fraction of a grid cell in LPJ-GUESS-SPITFIRE using an example 50% burned area detected by L3JRC.

BGD
5, 3091–3122, 2008

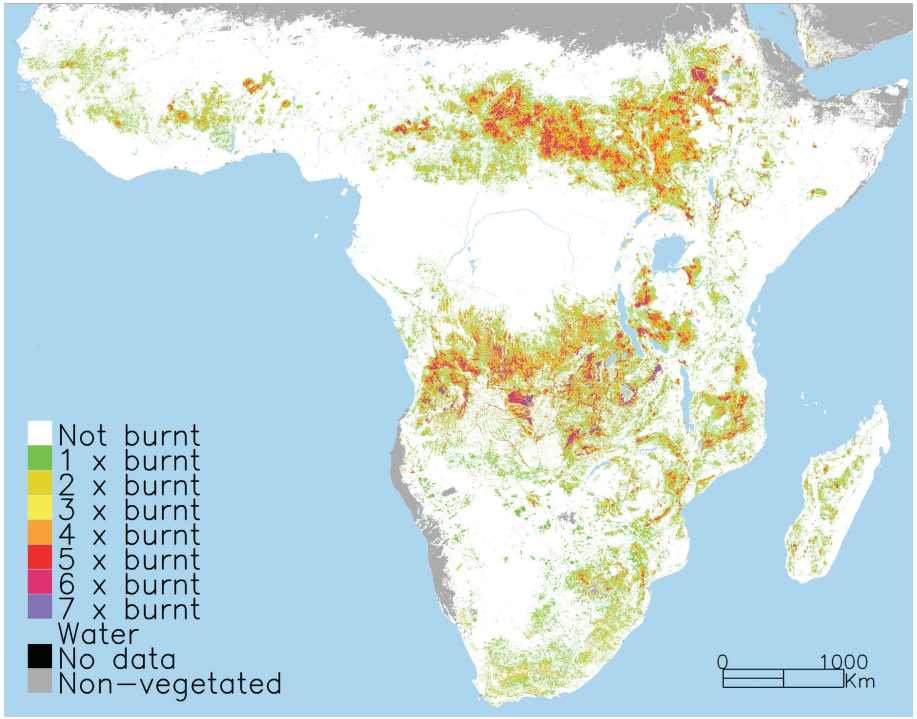

Fig. 2. Frequency and spatial extent of burned area covering a seven year period between 1 April 2000 and 31 March 2007 in sub-Saharan Africa according to the satellite-based burnt area map L3JRC.

BGD
5, 3091–3122, 2008

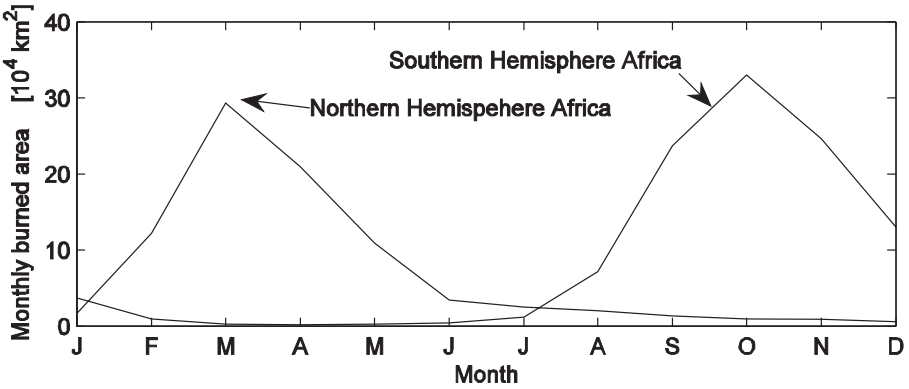

Fig. 3. Seasonality of burned area for northern and Southern Hemisphere Africa as estimated by L3JRC (mean values for 2001–2006). The total amount of burned area in the southern part of the continent exceeds the burnt area in the northern part by ca 20%.

BGD
5, 3091–3122, 2008

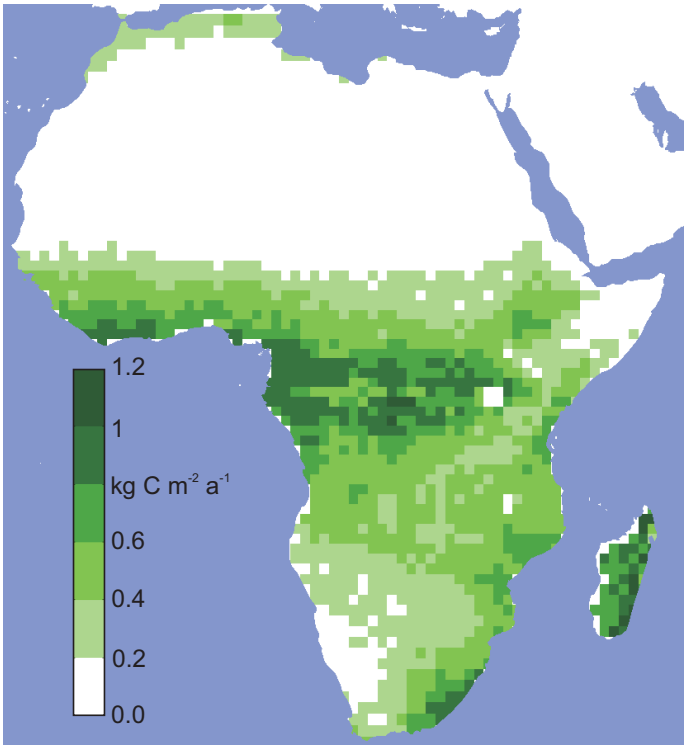

Fig. 4. Average annual net primary production in kg C m^{-2} a^{-1} for the period 2001 to 2006 simulated by LPJ-GUESS-SPITFIRE.

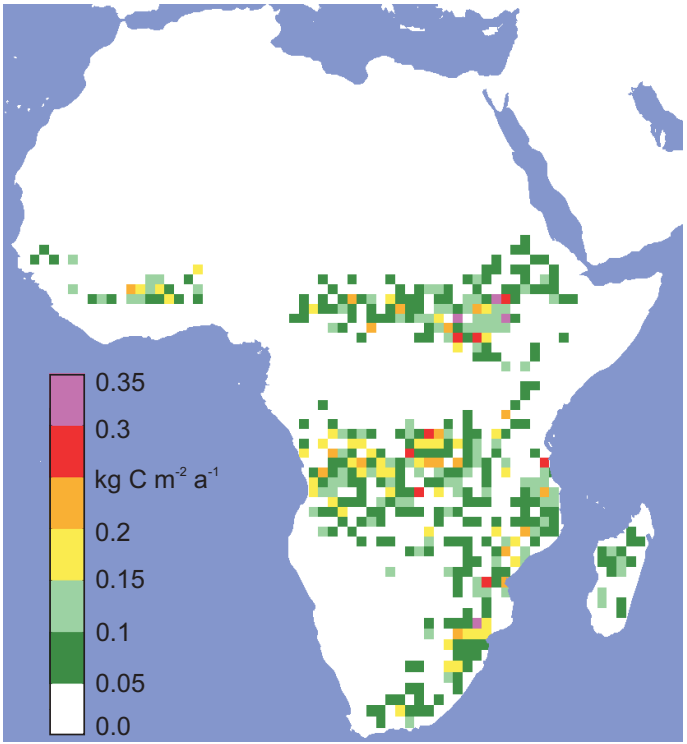

Fig. 5. Average total annual C emissions by wildfires expressed as kg C m^{-2} for the period 2001 to 2006 simulated by LPJ-GUESS-SPITFIRE with burnt area prescribed from L3JRC.

BGD
5, 3091–3122, 2008

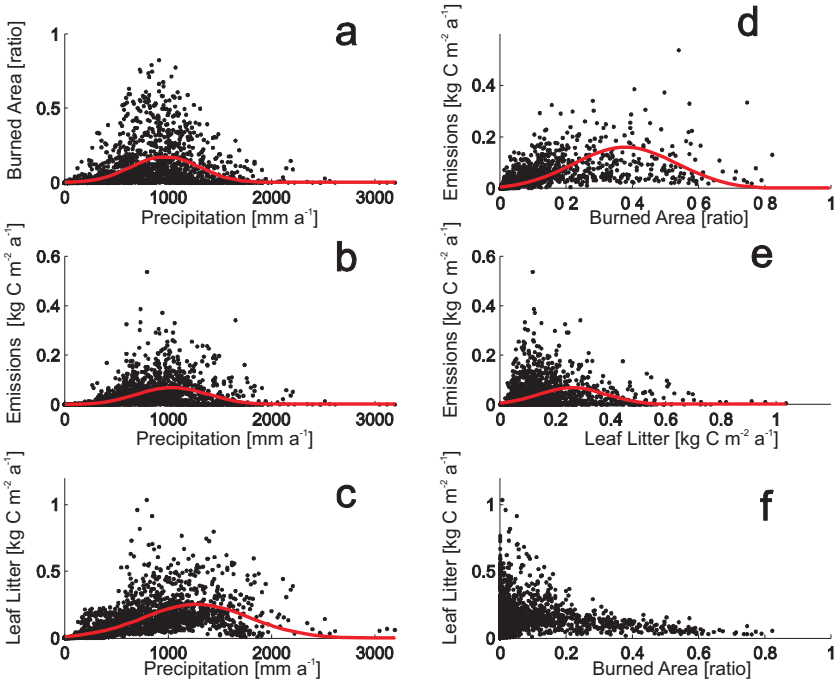

Fig. 6. The relationship between precipitation (prec), burned area (BA; expressed as fraction of a gridcell burnt), leaf litter (Lit) and emissions (E). Emission and burned area are scaled by dividing by 1 kg C and 10 kg C respectively for the estimation of the GLMs. All values are mean values for a 1degree cell from 2000–2006. Red curves are fitted GLM's with the following parameters:

(a) logit (BA)=–0.0065+1.02 10^{-5} Prec–5.27 10^{-9} $Prec^2$ (r^2=0.51)

(b) logit (E)=–0.00347+0.145 Prec–3.55 $Prec^2$ (r^2=0.51)

(c) logit (Lit/10)=–0.0068+4.9210^{-6} Prec–1.9210^{-9} $Prec^2$ (r^2=0.63)

(d) logit (E)=–0.0051+0.018 BA–0.024 BA^2 (r^2=0.66)

(e) logit (E)=–0.00511+0.189 Lit/10–3.58 $(Lit/10)^2$ (r^2=0.37).